



## Pd–Cu/AC and Pt–Cu/AC catalysts for nitrate reduction with hydrogen: Influence of calcination and reduction temperatures

O.S.G.P. Soares<sup>a</sup>, J.J.M. Órfão<sup>a</sup>, J. Ruiz-Martínez<sup>b</sup>, J. Silvestre-Albero<sup>b</sup>, A. Sepúlveda-Escribano<sup>b</sup>, M.F.R. Pereira<sup>a,\*</sup>

<sup>a</sup> Laboratório de Catálise e Materiais (LCM), Laboratório Associado LSRE/LCM, Departamento de Engenharia Química, Faculdade de Engenharia, Universidade do Porto, Rua Dr. Roberto Frias, 4200-465 Porto, Portugal

<sup>b</sup> Laboratorio de Materiales Avanzados, Instituto Universitario de Materiales de Alicante, Departamento de Química Inorgánica, Universidad de Alicante, Apartado 99, E-03080 Alicante, Spain

### ARTICLE INFO

#### Article history:

Received 17 March 2010

Received in revised form 31 July 2010

Accepted 25 August 2010

#### Keywords:

Nitrate reduction

Activated carbon

Bimetallic catalysts

Preparation conditions

### ABSTRACT

The influence of calcination and reduction temperatures on the catalytic properties of Pd–Cu and Pt–Cu bimetallic catalysts supported on activated carbon for the reduction of nitrates was studied. The catalysts were prepared using different calcination and reduction temperatures, and the respective activities and selectivities for the reduction of nitrates in water with hydrogen were assessed. It was found that the different preparation conditions lead to different catalytic performances. For both catalysts, the activity decreases by increasing calcination and reduction temperatures, whereas the effect on the selectivity is not uniform. For the 1%Pd–0.3%Cu (wt.%) catalyst, the nitrate conversion after 5 h of reaction varies from 93% (sample calcined at 200 °C and not reduced) to 25% (sample calcined and reduced at 400 °C). The formation of alloys during the preparation of the catalysts is prejudicial for nitrate reduction. In all the preparation conditions tested the Pd–Cu pair is more selective for the transformation of nitrate into nitrogen. All the samples have been characterized by nitrogen adsorption at –196 °C, CO adsorption microcalorimetry, TPR, XRD, XPS and TEM.

© 2010 Elsevier B.V. All rights reserved.

### 1. Introduction

Nitrate concentrations in surface water, and especially in groundwater, have increased recently in many locations in the world, including Europe. The catalytic reduction with hydrogen has been suggested in the literature as a promising method for nitrate removal from water, without the drawbacks of the conventional methods [1,2]. This process was reported for the first time by Vorlop and Tacke [3], and consists in the reduction of nitrate to nitrogen over bimetallic catalysts in the presence of a reducing agent. The formation of nitrite as intermediate and ammonium as by-product is considered the main disadvantage of this process [2]. Previous studies on the heterogeneous catalytic nitrate reduction have shown that bimetallic catalysts are much more efficient than the monometallic ones. The catalyst is usually composed of a noble metal, mainly Pd or Pt but also Ru, Rh or Ir, and a promoter metal, such as Cu, Sn, Ag, Ni, Fe or In on different supports (alumina [4–10], silica [11–13], titania [14–16], activated carbon [17–24], niobia [25], hydrotalcite [26,27], ceria [28,29], tin oxide [30,31], polymers [32–35]). Among them, Pd–Cu, Pd–Sn and Pt–Cu seem to

be the most effective, but are still inadequate in terms of selectivity to nitrogen [19,24]. The activity and selectivity of the bimetallic catalyst are highly dependent on the interaction between the metals, and this can be controlled by the preparation method, the nature of the promoter, the metal/promoter ratio and the operation conditions [36]. Alloying of metals may result in important changes in their activities and selectivities [9]. Segregation phenomena of the metal phases can occur during the preparation of the catalysts. The metal of lower energy of sublimation tends to migrate to the surface. However, this surface enrichment with one of the two metals depends on a large number of parameters, such as the interactions of the metal with the support and the preparation and activation methods [9]. The selection of the support is also important for this process, since it has been shown that the support may affect the catalytic activity and selectivity [36].

Epron et al. [9] investigated the influence of oxidizing and reduction treatments, at ambient temperature or at 400 °C, in a bimetallic Pt–Cu catalyst supported on alumina. They concluded that the catalytic activity for nitrate reduction in water is dependent on the Pt and Cu distribution on the catalyst surface, which is strongly affected by the pre-treatments. In a more recent work, Sá et al. [37] studied the influence of the reduction temperature in the performance of a Pd–Cu catalysts supported on alumina, and they also observed significant changes in the catalytic activity. Gavagnin et al.

\* Corresponding author. Tel.: +351 225 081 468; fax: +351 225 081 449.  
E-mail address: [fpereira@fe.up.pt](mailto:fpereira@fe.up.pt) (M.F.R. Pereira).

[31] reported that ZrO<sub>2</sub> and SnO<sub>2</sub> can be used as supports for Pd–Cu in the nitrate reduction, and the activities and selectivities of the catalyst can be improved by decreasing the reduction temperature. Gao et al. [16] observed that Pd–Cu catalysts supported on titanium dioxide and treated at high temperatures (873 K) exhibit lower activity than non-thermally treated catalysts, probably because of the aggregation of active metal species caused by the high temperature treatment.

Activated carbons have been used in heterogeneous catalysis, both as catalysts on their own or as catalyst support. It has been proved that they have a great potential as catalyst support, especially for the expensive noble metals, since a high metal loading and dispersion can be achieved. Furthermore, the interaction between the active phase and the support can improve the catalytic activity [38]. In the present work, the influence of different calcination and reduction temperatures on the catalytic behaviour of activated carbon supported Pd–Cu and Pt–Cu bimetallic catalysts in the hydrogen-mediated reduction of nitrates in water has been studied.

## 2. Experimental

### 2.1. Catalysts preparation

The active metals were supported on a commercial activated carbon, NORIT GAC 1240 PLUS (ACo), ground to a particle diameter between 0.1 mm and 0.3 mm. The catalysts were prepared by incipient wetness co-impregnation, from aqueous solutions of the corresponding metal salts (H<sub>2</sub>PtCl<sub>6</sub>, PdCl<sub>2</sub>, Cu(NO<sub>3</sub>)<sub>2</sub>). During the impregnation, the samples were placed in an ultrasonic bath. Then, the samples were dried at 100 °C for 24 h. Different temperatures were selected for calcination ( $T_{\text{Cal}}$ ) under a nitrogen flow for 1 h, and reduction ( $T_{\text{Red}}$ ) under hydrogen flow for 3 h. No calcined and no reduced catalysts ( $N_{\text{Cal}}$   $N_{\text{Red}}$ ) were also studied; however, these samples could be considered calcined in air at 100 °C, once they were dried in the oven during their preparation. The contents of noble and promoter metals were maintained constant at 1 wt.% and 0.3 wt.%, respectively. For the pair Pd–Cu the composition 2 wt.% of Pd and 1% of Cu was also checked.

### 2.2. Catalysts characterization

The catalysts were characterized using different techniques: N<sub>2</sub> adsorption at –196 °C, temperature programme reduction (TPR), transmission electron microscopy (TEM), CO adsorption microcalorimetry, X-ray diffraction (XRD) and X-ray photoelectron spectroscopy (XPS).

The textural characterization of the materials was based on the corresponding N<sub>2</sub> adsorption isotherms, determined at –196 °C with a Coulter Omnisorp 100 CX apparatus. BET surface areas ( $S_{\text{BET}}$ ) were calculated, as well as the micropore volumes ( $V_{\text{micro}}$ ) and mesopore surface areas ( $S_{\text{meso}}$ ) according to the *t*-method.

TPR experiments were carried out in a AMI-200 (Altamira Instruments) apparatus; the sample (150 mg) was heated at 5 °C/min up to 600 °C under a flow of 5% (v/v) H<sub>2</sub> diluted in He (total flow rate of 30 Ncm<sup>3</sup>/min). The H<sub>2</sub> consumption was followed by a thermal conductivity detector (TCD) and by mass spectrometry (Dymaxion 200 amu, Ametek).

TEM analyses were obtained using a LEO 906E microscope operating at a 120 kV accelerating voltage.

Microcalorimetric measurements were performed at 25 °C using a Setaram BT.15D heat-flux calorimeter. The calorimeter was connected to a volumetric system employing a Baratron capacitance manometer for precision pressure measurement ( $\pm 0.001$  Torr). The maximum leak rate of the volumetric system (including the calorimetric cell) was 10<sup>–5</sup> Torr/min in a system vol-

ume of approximately 60 cm<sup>3</sup>. The catalysts (between 0.15 g and 0.5 g) were calcined for 1 h and reduced for 3 h in a special cell with high purity helium and hydrogen (50 Ncm<sup>3</sup>/min), respectively. After reduction, the sample was out-gassed at the reduction temperature for 15 min, and then purged at the same temperature for 1 h in high purity helium to remove any adsorbed hydrogen. Then, it was sealed in a Pyrex NMR tube and placed in a special calorimetric cell. When thermal equilibrium was reached, the capsule was broken, and small pulses of CO were introduced until saturation was achieved. The resulting heat response for each pulse was recorded as a function of time and integrated to determine the energy released. The differential heat (kJ/mol) was defined as the negative of the enthalpy change of adsorption per mole of gas adsorbed.

XRD spectra were recorded on a PANalytical X'Pert PRO diffractometer with Cu K $\alpha$  radiation source ( $\lambda = 0.154$  nm) and with a beam voltage of 50 kV and 40 mA of beam current. The data were collected in the  $2\theta$  range of 10–90° with a scanning rate of 0.017°/s.

XPS analyses were performed with a VG Scientific ESCALAB 200 A spectrometer using a non-monochromatised Mg K $\alpha$  radiation (1253.6 eV). The pressure in the analysis chamber was always lower than  $1 \times 10^{-7}$  Pa. The charging effects were corrected using the C1s peak, which was fixed on all samples at a binding energy (BE) of 285 eV. XPS data were fitted using the software XPSpeak.

### 2.3. Catalysts evaluation

The catalytic tests were carried out in a semi-batch reactor, equipped with a magnetic stirrer and a thermostatic jacket, at room temperature and atmospheric pressure, and using hydrogen as reducing agent. Initially, 790 mL of deionised water and 400 mg of catalyst were fed into the reactor, the magnetic stirrer was adjusted to 700 rpm and the gas mixture of hydrogen and carbon dioxide (1:1, flow rate = 200 Ncm<sup>3</sup>/min) was passed through the reactor during 15 min to remove oxygen; CO<sub>2</sub> acts as pH buffer (pH = 5.5). After that period, 10 mL of a nitrate solution, prepared from NaNO<sub>3</sub>, was added to the reactor, in order to obtain an initial NO<sub>3</sub><sup>–</sup> concentration equal to 100 ppm. Preliminary studies were carried out varying the stirring rate and it was checked that under the selected conditions there was no external diffusional limitations.

Small samples were taken from the reactor for determination of nitrate, nitrite and ammonium concentrations after defined periods. Nitrate and nitrite ions were simultaneously determined by HPLC using a Hitachi Elite Lachrom apparatus equipped with a diode array detector. The stationary phase was a Hamilton PRP-X100 column (150 mm  $\times$  4.1 mm) working at room temperature under isocratic conditions. The mobile phase was a 0.1 M solution of NaCl:CH<sub>3</sub>OH (45:55). Ammonium ions were determined by potentiometry using a convenient selective electrode. pH values were also measured.

The dissolved amounts of Pd, Pt and Cu were measured by atomic absorption spectroscopy, using the remaining solution after reaction tests. No leaching of Pd or Pt was detected at the end of the reaction, but in some experiments small amounts of dissolved Cu were observed in the solution. For example, for the catalyst 2%Pd–1%Cu.ACo a concentration of 0.327 mg/L of Cu was detected in the case of the sample  $N_{\text{Cal}}$   $N_{\text{Red}}$ , corresponding to a leaching of 7%, which was the highest value measured; this value decreases to 0.6% for the catalyst  $T_{\text{Cal}} = 400$  °C  $T_{\text{Red}} = 400$  °C. On the contrary, in the case of Pt–Cu catalysts no dissolved Cu was measured for the sample  $N_{\text{Cal}}$   $N_{\text{Red}}$ .

The selectivities of nitrite, ammonium and nitrogen were calculated as:

$$S_{\text{NO}_2^-} = \frac{n_{\text{NO}_2^-}}{n_{\text{NO}_3^-} - n_{\text{NO}_3^-}} \quad (1)$$

$$S_{\text{NH}_4^+} = \frac{n_{\text{NH}_4^+}}{n_{\text{NO}_3^-} - n_{\text{NO}_2^-}} \quad (2)$$

$$S_{\text{N}_2} = \frac{2 \times n_{\text{N}_2}}{n_{\text{NO}_3^-} - n_{\text{NO}_2^-}} \quad (3)$$

where  $n_{\text{NO}_3^-}$  is the initial amount of nitrate (mmol) and  $n_{\text{NO}_3^-}$ ,  $n_{\text{NO}_2^-}$ ,  $n_{\text{NH}_4^+}$  and  $n_{\text{N}_2}$  are the amounts of the respective species (mmol) at time  $t$  (min). The amounts of nitrogen were calculated by a mole balance, assuming that the  $\text{NO}_x$  produced is negligible.

### 3. Results and discussion

#### 3.1. Catalysts characterization

##### 3.1.1. Textural properties

Textural properties obtained from the  $\text{N}_2$  adsorption isotherms at  $-196^\circ\text{C}$  show that the support has a BET surface area of  $869\text{ m}^2/\text{g}$ , a mesopore surface area of  $97\text{ m}^2/\text{g}$  and a micropore volume of  $0.32\text{ cm}^3/\text{g}$ . It was previously verified that the textural parameters remained almost unchanged compared to the unloaded carbon when higher metal loads were used in this same activated carbon as a support [23]. Therefore, it is assumed that the textural properties of the supported metal catalysts are not significantly different from the original activated carbon.

##### 3.1.2. TPR

The TPR profiles (not shown) of the monometallic catalysts show peaks at  $190^\circ\text{C}$  for Pd,  $230^\circ\text{C}$  for Cu and  $200^\circ\text{C}$  for Pt. The reduction peak at around  $60^\circ\text{C}$  relative to the decomposition of Pd  $\beta$ -hydride [31,39,40] was not observed, which may indicate that Pd is well dispersed on the support [41]. The Pd–Cu catalyst showed a single reduction peak at  $150^\circ\text{C}$  that can be assigned to the reduction of Cu oxides, promoted by the presence of the noble metal [32,39,41]. The decrease in the reduction temperature of supported copper in bimetallic catalysts induced by the presence of palladium indicates that a close proximity between copper and palladium species was achieved [41]. The TPR profile of the Pt–Cu catalyst is characterized by two peaks at  $200^\circ\text{C}$  and  $400^\circ\text{C}$ . The first one, located around that of the pure platinum catalyst, indicates the reduction of mixed Pt–Cu oxidized species where both metals are in close contact. The peak at higher temperatures could be attributed to the reduction of isolated copper species [6]. Supported CuO may be reduced at higher temperatures depending on the particle size and its interaction with the support [42]. It could be assumed that oxidized copper particles in the bimetallic catalyst are well dispersed and interact strongly with the support, which is the most probable explanation for their reduction at higher temperature than the monometallic copper particles [9].

##### 3.1.3. TEM

TEM analyses were made in order to get information on the particle size distribution for all samples. TEM images and the corresponding histograms of the particle size distributions (Figs. 1–3) revealed that the average particle size depends on the calcination/reduction conditions. In both series (Pd–Cu and Pt–Cu), the evolution of the particle size with the temperatures used during calcination/reduction presents a similar trend (Figs. 1 and 3). No major differences were observed in the morphology of the catalysts neither calcined nor reduced; in fact, in this sample, no particles can be detected (Fig. 3a), due to the fact that this catalyst was not heat treated and, consequently, no metal particles were generated, or the particles have a diameter lower than 2 nm (detection limit of the equipment used). For the catalysts  $T_{\text{Cal}} = 200^\circ\text{C}$   $T_{\text{Red}} = 100^\circ\text{C}$  (Figs. 1a, 2 and 3b) only a few particles can be observed. In the

case of 1%Pd–0.3%Cu.ACo  $T_{\text{Cal}} = 200^\circ\text{C}$   $T_{\text{Red}} = 100^\circ\text{C}$  (Fig. 1b) and 1%Pt–0.3%Cu.ACo  $T_{\text{Cal}} = 200^\circ\text{C}$   $T_{\text{Red}} = 100^\circ\text{C}$  (Fig. 3c) it is already possible to see a significant number of well defined particles. These observations suggest that metals are well dispersed on the support. From the particle size distributions it was observed that these catalysts mainly present particle sizes between 3 nm and 4 nm and only a few particles higher than 5 nm were detected in some of them. For the 1%Pd–0.3%Cu.ACo and 1%Pt–0.3%Cu.ACo catalysts with  $T_{\text{Cal}} = 200^\circ\text{C}$   $T_{\text{Red}} = 200^\circ\text{C}$  and  $T_{\text{Cal}} = 400^\circ\text{C}$   $T_{\text{Red}} = 400^\circ\text{C}$ , TEM analyses show the presence of not only small particles in the range of 5–6 nm, but also many larger particles (see Figs. 1c, 3d and e).

From the TEM micrographs it can be concluded that calcination and reduction at different temperatures lead to significant changes in the average particle size. As can be seen in the histograms, an increase in the calcination and reduction temperatures causes an increase in the particle size of the crystallites. These results are in agreement with those reported by Gurrath et al. [40] and Ramos et al. [43] for Pd supported on activated carbons. These authors observed that reduction at higher temperatures originates a decrease in the dispersion, which should be attributed to an increase in the metallic particle size due to the migration of particles and sintering during the calcination and reduction steps [43]. Sepúlveda-Escribano et al. [44] observed the same effect for Pt supported on carbon blacks. The increase of the particle size can also be promoted by the thermal decomposition of the oxygenated surface groups initially present on the activated carbon surface. With the destruction of these groups, the fixed small metal particles (or the unreduced precursor) would become mobile on the surface and consequently would agglomerate to larger particles [44,45].

##### 3.1.4. CO adsorption microcalorimetry

This technique can give information about the energetic interaction of CO with the different surface metals, which allows to assess the heterogeneity of the surface and the interaction between metals. Since CO hardly adsorb on copper [46], only CO adsorption on either Pt or Pd was considered. Small doses of CO were contacted with the reduced catalysts and the differential heat of adsorption was measured as a function of the CO coverage.

Fig. 4 shows the differential heat of CO adsorption at  $25^\circ\text{C}$  as a function of the coverage for the monometallic Pd and 1%Pd–0.3%Cu.ACo catalysts after different calcination/reduction treatments. For the monometallic catalyst, the initial heat is around  $190\text{ kJ/mol}$ , and it strongly decreases with the CO coverage up to  $40\ \mu\text{mol/g}$ , where a plateau was reached. The CO coverage was similar in the 1%Pd–0.3%Cu.ACo with  $T_{\text{Cal}} = 200^\circ\text{C}$   $T_{\text{Red}} = 100^\circ\text{C}$ ; therefore, Cu is not blocking the Pd sites where the CO is adsorbed. Moreover, the heat of adsorption profiles is roughly the same in both catalysts, so the energetic interaction of CO with Pd has not changed with the addition of Cu.

Different results are obtained with the 1%Pd–0.3%Cu.ACo catalyst using  $T_{\text{Cal}} = 200^\circ\text{C}$   $T_{\text{Red}} = 200^\circ\text{C}$ . These changes in the profile show up important modifications in the Pd active sites by effect of the reduction temperature. The initial heat of adsorption is now  $99\text{ kJ/mol}$ , and slightly decreases with the CO coverage; furthermore, the amount of CO adsorbed has also decreased with respect to its counterparts. The lower energetic interaction of CO with Pd active sites suggests that Cu is modifying Pd. These effects are even more clear after a calcination and reduction treatment at high temperature ( $T_{\text{Cal}} = 400^\circ\text{C}$   $T_{\text{Red}} = 400^\circ\text{C}$ ), where the lower energetic interaction of CO with Pd is also accompanied by a drastic decrease in the amount of CO adsorbed. Either the sintering of the Pd nanoparticles and/or, more likely, the dilution of surface Pd by Cu (large migration of Cu to surface positions after a high temperature reduction treatment), with possible Pd–Cu alloy formation, may account for the observed behaviour. Earlier investigations [47] on the interaction of CO with Pd–Cu alloys have shown a decrease

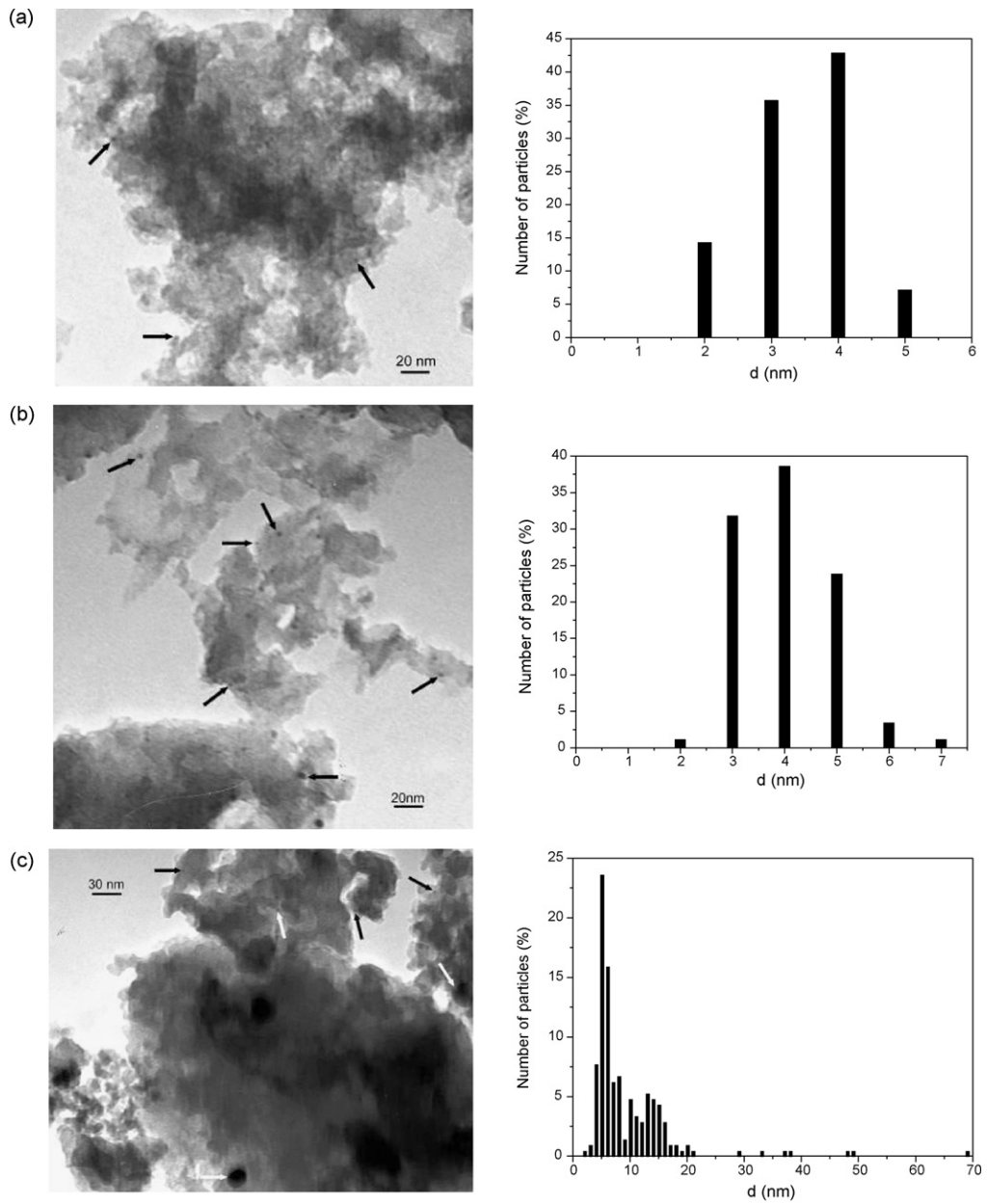


Fig. 1. TEM micrographs and particles size distributions of 1%Pd-0.3%Cu\_ACo catalysts: (a)  $T_{Cal} = 200\text{ }^{\circ}\text{C}$   $N_{Red}$ , (b)  $T_{Cal} = 200\text{ }^{\circ}\text{C}$   $T_{Red} = 100\text{ }^{\circ}\text{C}$  and (c)  $T_{Cal} = 400\text{ }^{\circ}\text{C}$   $T_{Red} = 400\text{ }^{\circ}\text{C}$ .

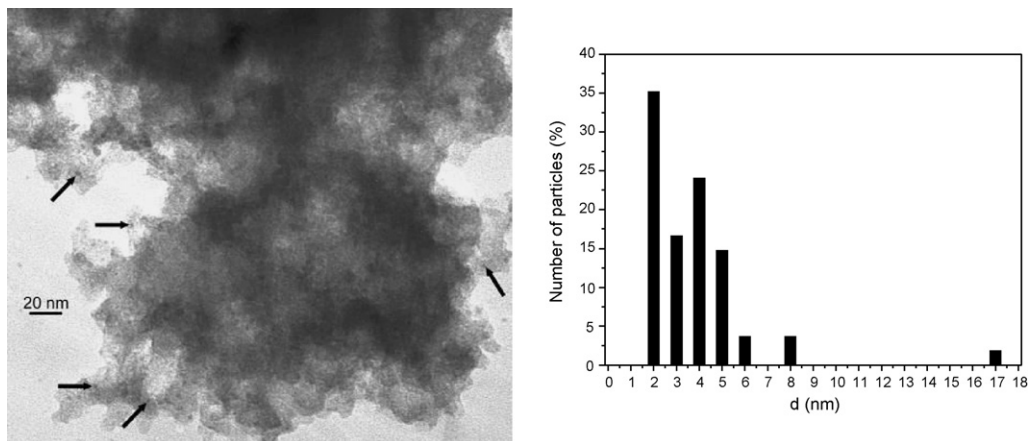
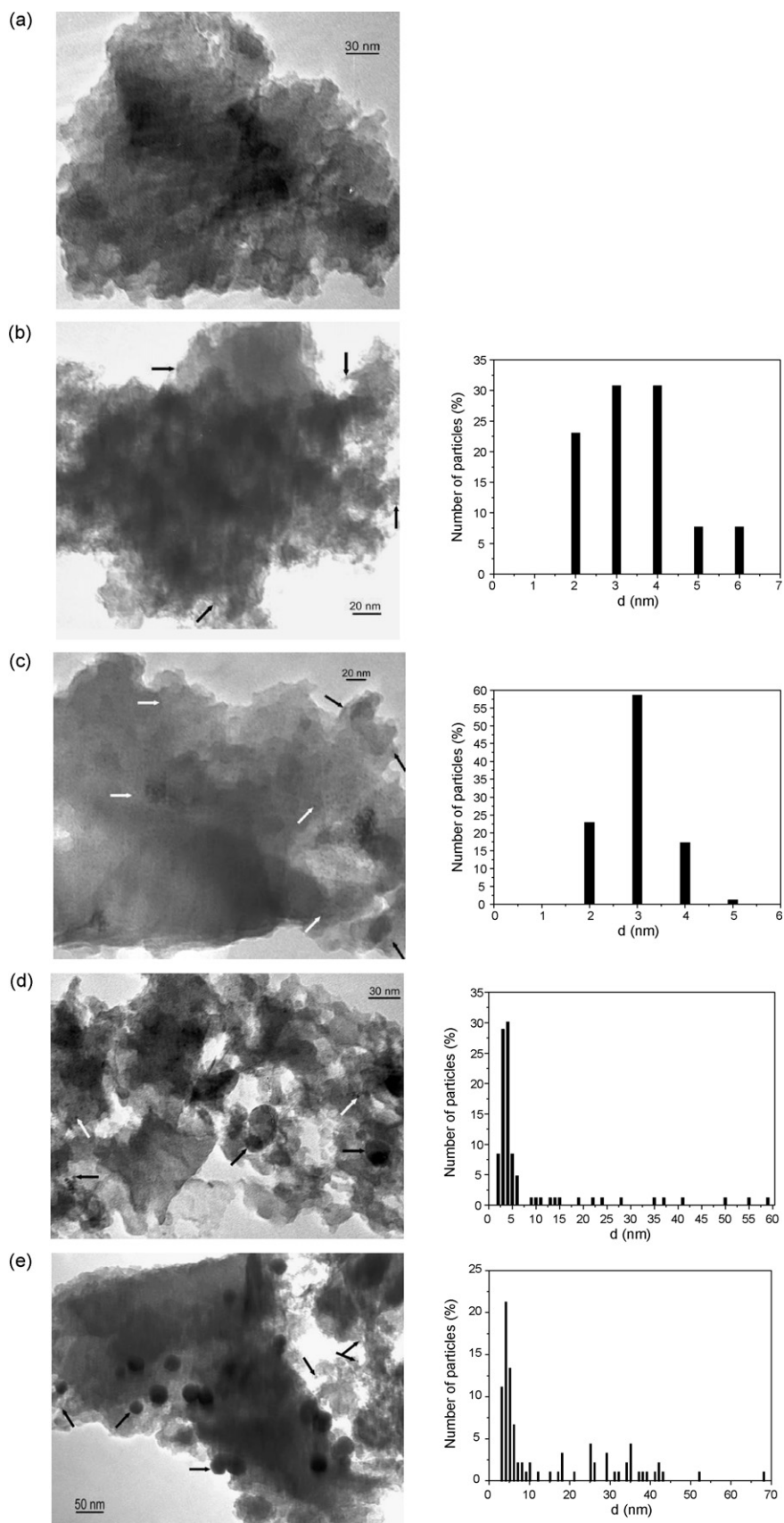
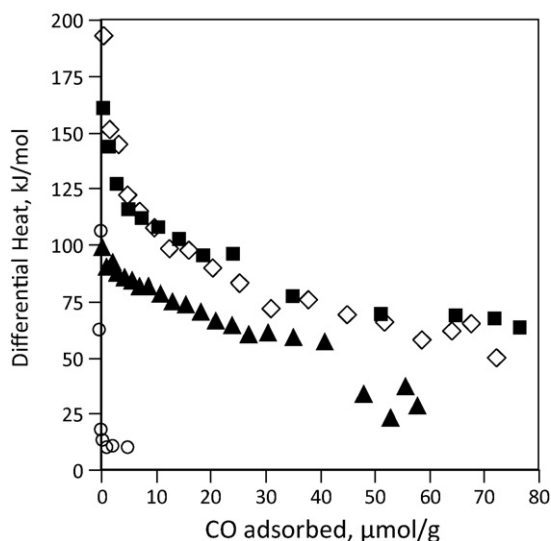


Fig. 2. TEM micrograph and particles size distribution of the 2%Pd-1%Cu\_ACo catalyst  $T_{Cal} = 200\text{ }^{\circ}\text{C}$   $N_{Red}$ .



**Fig. 3.** TEM micrographs and particles size distributions of 1%Pt-0.3%Cu-ACo catalysts: (a)  $N_{\text{Cal}}$   $N_{\text{Red}}$ , (b)  $T_{\text{Cal}} = 200^\circ\text{C}$   $N_{\text{Red}}$ , (c)  $T_{\text{Cal}} = 200^\circ\text{C}$   $T_{\text{Red}} = 100^\circ\text{C}$ , (d)  $T_{\text{Cal}} = 200^\circ\text{C}$   $T_{\text{Red}} = 200^\circ\text{C}$  and (e)  $T_{\text{Cal}} = 400^\circ\text{C}$   $T_{\text{Red}} = 400^\circ\text{C}$ .





**Fig. 4.** Differential heats of adsorption as a function of CO coverage at 25 °C on the monometallic Pd<sub>1</sub>Co (◇), on 1%Pd–0.3%Cu<sub>0.3</sub>Co  $T_{\text{Cal}}=200\text{ }^{\circ}\text{C}$   $T_{\text{Red}}=100\text{ }^{\circ}\text{C}$  (■);  $T_{\text{Cal}}=200\text{ }^{\circ}\text{C}$   $T_{\text{Red}}=200\text{ }^{\circ}\text{C}$  (▲) and  $T_{\text{Cal}}=400\text{ }^{\circ}\text{C}$   $T_{\text{Red}}=400\text{ }^{\circ}\text{C}$  (○).

in the CO interaction with the amount of Cu. Fernández-García et al. [48] and Anderson et al. [49] observed a decrease in the number of CO molecules bridging two or more Pd atoms, which are the most energetic sites for CO adsorption [50], when Cu was added, indicating a dilution of the surface Pd by Cu, which also correlates with the loss in the adsorption capacity.

The heat of CO adsorption profiles for the Pt catalysts are plotted in Fig. 5. The low CO adsorption capacity of this catalyst complicates the analysis, since only few doses can be introduced. Nevertheless, the amount of CO adsorbed and the heat of adsorption on the bimetallic 1%Pt–0.3%Cu<sub>0.3</sub>Co with  $T_{\text{Cal}}=200\text{ }^{\circ}\text{C}$   $T_{\text{Red}}=200\text{ }^{\circ}\text{C}$  is lower than on the monometallic one in all the range of coverage. This effect, as in the Pd–Cu catalyst, would be most likely due to the formation of a Pt–Cu alloy. Copper in metallic state is diluting and interacting with the surface Pt atoms, thus decreasing the number of Pt active sites and their interaction with CO. Li et al. [51] found analogous results on Pt–Cu catalysts supported on SiO<sub>2</sub> for both, H<sub>2</sub> and CO adsorption.

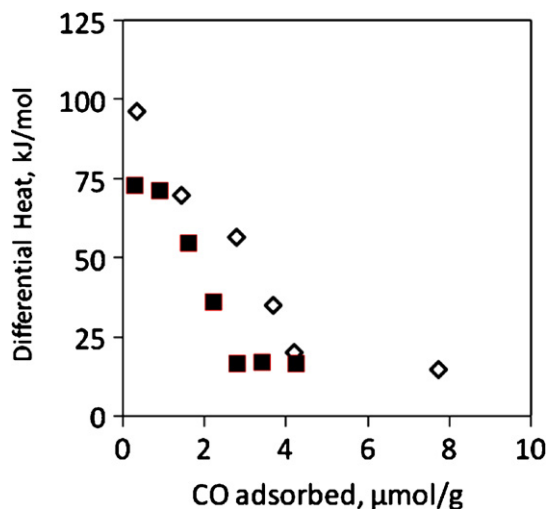


**Fig. 5.** Differential heats of adsorption as a function of CO coverage at 25 °C on the monometallic Pt<sub>1</sub>Co (◇) and on 1%Pt–0.3%Cu<sub>0.3</sub>Co  $T_{\text{Cal}}=200\text{ }^{\circ}\text{C}$   $T_{\text{Red}}=200\text{ }^{\circ}\text{C}$  (■).

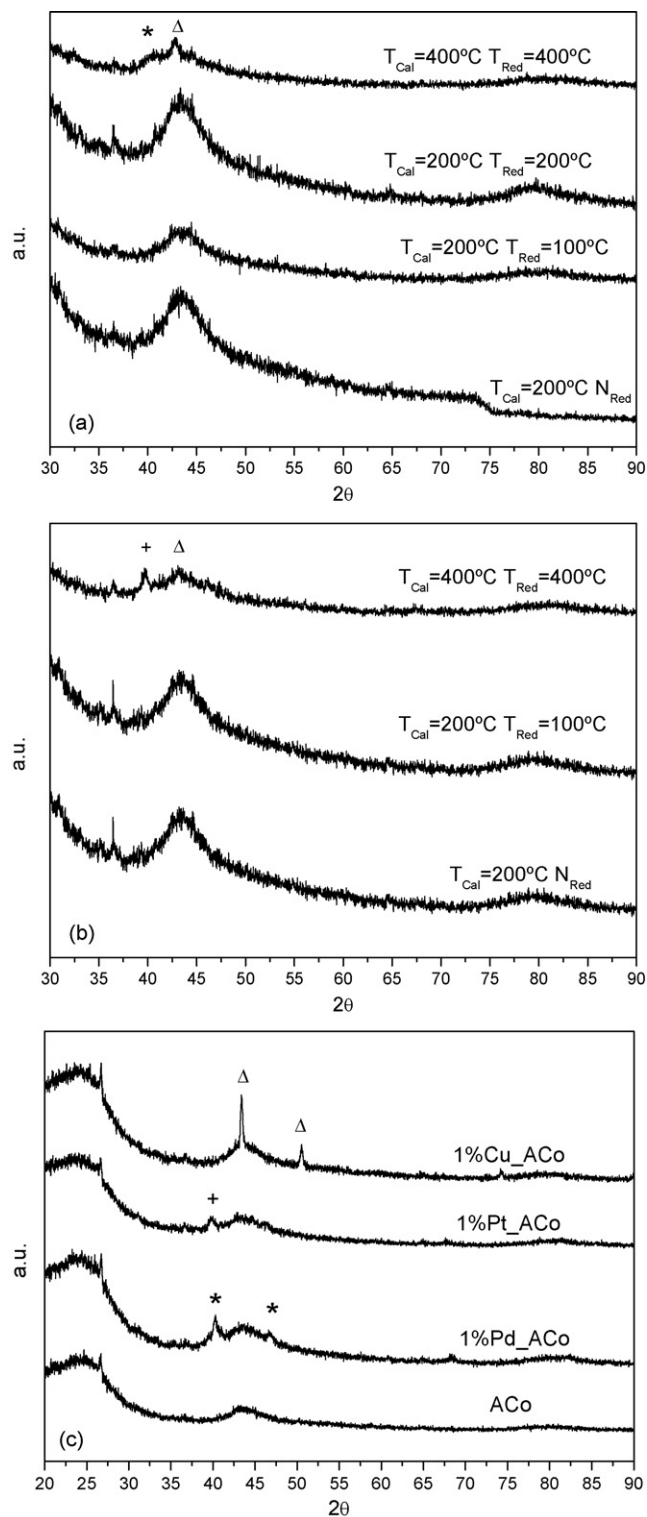


**Fig. 6.** XRD spectra of (a) 1%Pd–0.3%Cu<sub>0.3</sub>Co, (b) 1%Pt–0.3%Cu<sub>0.3</sub>Co catalysts and (c) monometallic catalysts  $T_{\text{Cal}}=400\text{ }^{\circ}\text{C}$   $T_{\text{Red}}=400\text{ }^{\circ}\text{C}$  and support (ACo). Copper (Δ), platinum (+), palladium (\*).

### 3.1.5. XRD

Fig. 6a and b shows the X-ray diffraction spectra of the 1%Pd–0.3%Cu<sub>0.3</sub>Co and 1%Pt–0.3%Cu<sub>0.3</sub>Co catalysts, respectively, calcined and reduced at different temperatures. The X-ray diffraction spectra of the support (ACo) and of the monometallic catalysts (1%Pd<sub>1</sub>Co, 1%Pt<sub>1</sub>Co and 1%Cu<sub>1</sub>Co) calcined and reduced at 400 °C, are reported in Fig. 6c.

**Table 1**  
XPS results for the 1%Pd–0.3%Cu.ACo catalysts.

Catalyst	Cu 2p <sub>3/2</sub> (eV)	Pd 3d <sub>5/2</sub> (eV)	Pd/Cu (at.) XPS
$N_{\text{Cal}} N_{\text{Red}}$	934.2	337.5	1.15
$T_{\text{Cal}} = 200\text{ }^{\circ}\text{C } N_{\text{Red}}$	934.1	337.5	1.09
$T_{\text{Cal}} = 200\text{ }^{\circ}\text{C } N_{\text{Red}}$ after 15 min under hydrogen flow in water	935.8	337.1	0.48
$T_{\text{Cal}} = 200\text{ }^{\circ}\text{C } N_{\text{Red}}$ after 5 h of reaction	935.1	337.9	0.26
$T_{\text{Cal}} = 200\text{ }^{\circ}\text{C } T_{\text{Red}} = 100\text{ }^{\circ}\text{C}$	935.1	337.6	1.50

The XRD profile of the support (ACo) shows two broad peaks centered around  $2\theta = 24^{\circ}$  and  $44^{\circ}$ , which are due to turbostratic carbon [52]. In 1%Pd–0.3%Cu.ACo and 1%Pt–0.3%Cu.ACo catalysts, the XRD spectra do not show any intense peak corresponding to the metals, which could be due to the low amount of metal loaded and, on the other hand, could be taken as an indication of a good metal dispersion on the support [31]. TEM observations support this last conclusion. Only in the XRD spectra of the bimetallic catalysts 1%Pd–0.3%Cu.ACo and 1%Pt–0.3%Cu.ACo with  $T_{\text{Cal}} = 400\text{ }^{\circ}\text{C}$   $T_{\text{Red}} = 400\text{ }^{\circ}\text{C}$  significant peaks corresponding to the metals can be observed, this being indicative of the presence of larger particles than when the catalysts are treated at lower temperatures, and is in agreement with the TEM analyses. In addition, in these XRD spectra it can be observed that the Pd and Pt peaks are slightly displaced to the right, which is indicative of the formation of alloys [31,32], as confirmed by CO adsorption microcalorimetry.

### 3.1.6. XPS

Concerning the XPS characterization, the objective was to estimate the relative abundance of the metals at the surface as a function of the calcination and reduction treatments. The information concerning their oxidation states must be considered with reserve because these experiments were not carried out *in situ*, therefore, some surface oxidation could result from the contact with air during sample manipulation. Besides the characterization by XPS of the fresh and the spent 1%Pd–0.3%Cu.ACo catalyst  $T_{\text{Cal}} = 200\text{ }^{\circ}\text{C } N_{\text{Red}}$ , an additional sample was prepared with the aim to understand the influence of the initial 15 min contact between the catalyst and hydrogen in water before starting reaction (addition of nitrate). The Pd 3d and Cu 2p spectra of the bimetallic samples were analysed and the binding energies of the Pd 3d<sub>5/2</sub> and Cu 2p<sub>3/2</sub> levels are reported in Table 1. The surface Pd/Cu atomic ratio, obtained by XPS, is also presented in Table 1.

Barrabés et al. [18] identified platinum, palladium and copper supported on activated carbon in the reduced form for the fresh catalysts, but for some of the used catalyst the metals were not only in the reduced form but also in the oxidized form. According to the TPR profiles, it was expected that the heat treated catalysts were in the reduced form. However, in this work, the binding energies values found for copper and palladium are respectively characteristic of Cu<sup>2+</sup> [53,54] and Pd<sup>2+</sup> [55,56], i.e. of the oxidized form. Probably, this is due to the contact with air after the calcination and/or reduction and after reaction, which could oxidise the metals [39]. In addition, according to Yamamoto et al. [57], in the samples calcined at 200 °C, the presence of copper prevents the reduction of Pd<sup>2+</sup> to Pd<sup>0</sup> due to a preferential reduction of Cu<sup>2+</sup> relatively to that of Pd<sup>2+</sup> on the reduction sites of activated carbon, due to the lower redox potential of Cu<sup>2+</sup> to Cu<sup>+</sup> (0.15 V vs. Ag<sup>+</sup>/AgCl) than that of Pd<sup>2+</sup> to Pd<sup>0</sup> (0.92 V). However, as can be seen in the next section, the contact with reaction media can change the surface of the catalysts, and although the metals are in the oxidized form they are reduced *in situ* during the kinetic experiments, where the catalysts are continuously in contact with hydrogen dissolved in water.

The increase in the Pd/Cu ratio with increasing of the reduction temperature can be explained by Cu migration. Epron et al. [9] proposed Cu migration during the reduction of Pt–Cu catalysts. The

migration was supposed to be towards the core of the bimetallic particles, leading to a surface enrichment with platinum, but also to a decrease in the amount of superficial copper. Moreover, according to Sá et al. [37], copper seems to migrate towards the support with the increase of the reduction temperature. These suggestions are consistent with our results.

Nevertheless, from the comparison between XPS results of the fresh and the spent catalyst  $T_{\text{Cal}} = 200\text{ }^{\circ}\text{C } N_{\text{Red}}$ , significant differences were observed in their surface composition after 15 min of contact with hydrogen in water and after 5 h of reaction, where a low Pd/Cu ratio is obtained. Considering that the measurements of leached metals for this sample indicate that no palladium was detected and that the amount of dissolved copper is very low, the decrease of this ratio is not due to leaching of the metals. Yoshinaga et al. [17] have also found that when activated carbon is used as a support for this reaction the dissolved amounts of Pd and Cu were negligibly small. Therefore, the results can only be explained by the modification of the copper and palladium relative distribution on the catalyst surface. This surface modification may be induced by the contact with the reaction media, which allows an rearrangement of the metal phases [9]. The decrease of the Pd/Cu ratio could be due to the preferential migration of palladium towards the interior of the support [40] and/or the migration of copper to the surface of palladium during reaction.

As can be seen in Table 1, the atomic ratio between Pd and Cu obtained by XPS is lower than the theoretical (1.99). This is related with the fact that XPS is a surface technique and then only gives an estimative of the chemical composition of the uppermost surface layers (about 10–15 nm in depth).

### 3.2. Catalytic tests

The effect of calcination and reduction temperatures on the catalytic activity and selectivity during the reduction of nitrates was studied. The activities of 1%Pd–0.3%Cu.ACo and 1%Pt–0.3%Cu.ACo catalysts are shown in Figs. 7a and 8a, respectively. Figs. 7b, 8b, 7c and 8c show the corresponding evolution of nitrite and ammonium concentrations during the reaction.

As can be seen in Figs. 7 and 8, the reduction of nitrates is quite different depending on the supported metal and the calcination/reduction conditions. In general, for the two catalysts, the activity decreases by increasing the calcination and reduction temperatures. This effect is more pronounced for the pair Pd–Cu. For high calcination and reduction temperatures, the Pt–Cu catalysts are more active than the Pd–Cu catalysts. However, using a low reduction temperature or not carrying out the reduction step, the Pd–Cu catalysts are the most active. The order of activity for both catalysts is similar:  $T_{\text{Cal}} = 200\text{ }^{\circ}\text{C } N_{\text{Red}} > N_{\text{Cal}} N_{\text{Red}} > T_{\text{Cal}} = 200\text{ }^{\circ}\text{C } T_{\text{Red}} = 100\text{ }^{\circ}\text{C} > T_{\text{Cal}} = 200\text{ }^{\circ}\text{C } T_{\text{Red}} = 200\text{ }^{\circ}\text{C} > T_{\text{Cal}} = 400\text{ }^{\circ}\text{C } T_{\text{Red}} = 400\text{ }^{\circ}\text{C}$ , with nitrate conversion values after 5 h of 93%, 85%, 79%, 35% and 25%, and 77%, 73%, 64%, 57% and 53%, respectively for the Pd–Cu and the Pt–Cu catalysts. For the 2%Pd–1%Cu.ACo catalysts the results are also similar; nevertheless, in this case, higher conversions are obtained. For example, 100% nitrate conversions were achieved for all the samples prepared at low temperatures (cf. Table 2), and for the best catalyst ( $T_{\text{Cal}} = 200\text{ }^{\circ}\text{C } N_{\text{Red}}$ ) before 200 min of reaction.

**Table 2**

Nitrate conversions ( $X_{\text{NO}_3^-}$ ) and nitrite, ammonium and nitrogen selectivities ( $S_{\text{NO}_2^-}$ ,  $S_{\text{NH}_4^+}$ ,  $S_{\text{N}_2}$ ) in the presence of Pd–Cu and Pt–Cu catalysts after 5 h of reaction and nitrogen selectivity for 25% and 50% nitrate conversions.

Catalyst (wt.%)	$t = 300 \text{ min}$				$S_{\text{N}_2}$	
	$X_{\text{NO}_3^-}$	$S_{\text{NO}_2^-}$	$S_{\text{NH}_4^+}$	$S_{\text{N}_2}$	$X_{\text{NO}_3^-} = 25\%$	$X_{\text{NO}_3^-} = 50\%$
<b>1%Pd–0.3%Cu.ACo</b>						
$N_{\text{Cal}} N_{\text{Red}}$	0.85	0.04	0.40	0.56	0.46	0.58
$T_{\text{Cal}} = 200^\circ\text{C} N_{\text{Red}}$	0.93	0.01	0.51	0.48	0.37	0.48
$T_{\text{Cal}} = 200^\circ\text{C} T_{\text{Red}} = 100^\circ\text{C}$	0.79	0.00	0.41	0.59	0.68	0.65
$T_{\text{Cal}} = 200^\circ\text{C} T_{\text{Red}} = 200^\circ\text{C}$	0.35	0.01	0.35	0.64	0.56	–
$T_{\text{Cal}} = 400^\circ\text{C} T_{\text{Red}} = 400^\circ\text{C}$	0.25	0.11	0.57	0.31	0.31	–
<b>2%Pd–1%Cu.ACo</b>						
$N_{\text{Cal}} N_{\text{Red}}$	1.00	0.00	0.39	0.61	0.49	0.51
$T_{\text{Cal}} = 200^\circ\text{C} N_{\text{Red}}$	1.00	0.00	0.57	0.43	0.21	0.32
$T_{\text{Cal}} = 200^\circ\text{C} T_{\text{Red}} = 100^\circ\text{C}$	0.99	0.00	0.35	0.65	0.67	0.70
$T_{\text{Cal}} = 200^\circ\text{C} T_{\text{Red}} = 200^\circ\text{C}$	0.91	0.01	0.30	0.69	0.65	0.70
$T_{\text{Cal}} = 400^\circ\text{C} T_{\text{Red}} = 400^\circ\text{C}$	0.61	0.02	0.59	0.39	0.36	0.39
<b>1%Pt–0.3%Cu.ACo</b>						
$N_{\text{Cal}} N_{\text{Red}}$	0.73	0.31	0.42	0.27	0.17	0.19
$T_{\text{Cal}} = 200^\circ\text{C} N_{\text{Red}}$	0.77	0.24	0.45	0.31	0.24	0.22
$T_{\text{Cal}} = 200^\circ\text{C} T_{\text{Red}} = 100^\circ\text{C}$	0.64	0.17	0.51	0.33	0.30	0.25
$T_{\text{Cal}} = 200^\circ\text{C} T_{\text{Red}} = 200^\circ\text{C}$	0.57	0.19	0.44	0.37	0.34	0.34
$T_{\text{Cal}} = 400^\circ\text{C} T_{\text{Red}} = 400^\circ\text{C}$	0.53	0.17	0.52	0.31	0.30	0.31

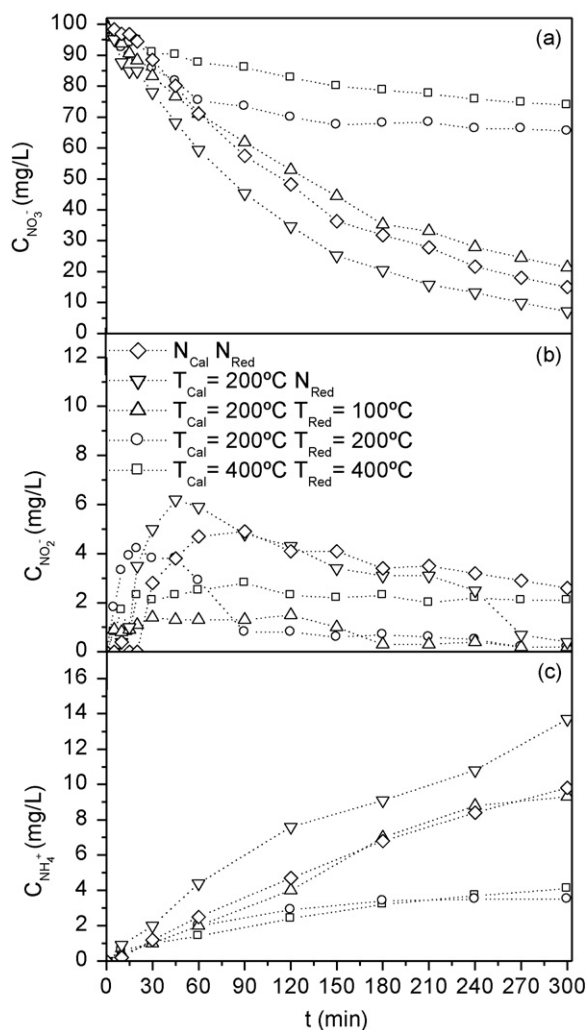


**Fig. 7.** (a)  $\text{NO}_3^-$ , (b)  $\text{NO}_2^-$  and (c)  $\text{NH}_4^+$  concentrations as a function of time during nitrate reduction in the presence of 1%Pd–0.3%Cu.ACo catalysts ( $C_{\text{NO}_3^-} = 100 \text{ mg/L}$ , catalyst = 0.5 g/L, pH = 5.5,  $Q_{\text{H}_2} = 100 \text{ Ncm}^3/\text{min}$ ,  $Q_{\text{CO}_2} = 100 \text{ Ncm}^3/\text{min}$ ,  $T = 25^\circ\text{C}$ ).

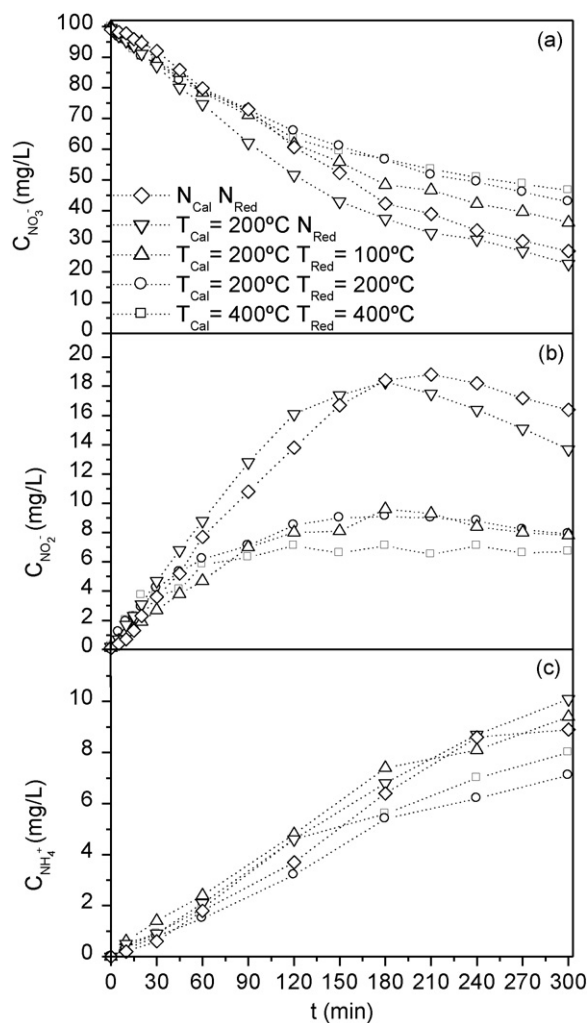


**Fig. 8.** (a)  $\text{NO}_3^-$ , (b)  $\text{NO}_2^-$  and (c)  $\text{NH}_4^+$  concentrations as a function of time during nitrate reduction in the presence of 1%Pt–0.3%Cu.ACo catalysts ( $C_{\text{NO}_3^-} = 100 \text{ mg/L}$ , catalyst = 0.5 g/L, pH = 5.5,  $Q_{\text{H}_2} = 100 \text{ Ncm}^3/\text{min}$ ,  $Q_{\text{CO}_2} = 100 \text{ Ncm}^3/\text{min}$ ,  $T = 25^\circ\text{C}$ ).



According to the TPR profiles, Pd–Cu and Pt–Cu bimetallic catalysts are reduced at around 150 °C and 200 °C, respectively. So, it was expected that the catalysts that have not been heat treated or have been treated at low temperatures were, after preparation, in the oxidized state. It is well assumed that the catalytic activity is related with several factors such as metals dispersion, preparation conditions, metals nature, type of support and, also, by the contact with hydrogen in water. In the next section, it will be demonstrated that the last factor plays an important role in the catalyst performance. This contact will originate some *in situ* reduction of the noble metal. Copper does not need to be in its reduced form in this catalytic system [9]. Epron et al. [9] studied the influence of oxidizing and reducing procedures on the activity of a Pt–Cu bimetallic catalyst supported on alumina, and they also observed that the poorest activity was achieved when the catalyst was oxidized and reduced at 400 °C. They concluded that this lower activity results from the destruction of the interactions between copper and platinum, and a subsequent migration of copper towards the alumina support. Therefore, a surface enrichment with platinum was noticed, which eventually decreases the catalytic activity. In the present work, the results obtained by XPS confirm an increase of the Pd content on the surface of the catalyst with the increase of calcination and reduction temperatures.

The nitrite concentration goes through a maximum (Figs. 7b and 8b) and the ammonium concentration increases with the nitrate conversion (Figs. 7c and 8c), according to the occurrence of consecutive/competitive reactions. The reduced catalysts give rise to similar nitrite concentrations which, particularly in the case of the Pt–Cu catalysts, are lower than the concentrations obtained with the non-reduced catalysts. This can be explained by the fact that for the catalysts only calcinated or not heat treated the active sites for nitrite reduction are not completely formed. As can be seen in the TEM micrographs, no or a limited number of particles were observed for these catalysts, indicating a good dispersion of the metals or, most probably, that the metal particles are still not completely formed after preparation (especially for the non heat treated sample). Therefore, in these conditions, the metal could not be very active for nitrite reduction. It is well assumed that nitrite reduction occurs principally on the monometallic sites of the noble metal [1,22].

A similar trend is observed for ammonia, but in this case the highest concentrations were measured for the Pd–Cu catalysts, certainly because the conversions attained with these catalysts are higher than in the presence of the Pt–Cu catalysts.

Considering that these catalysts have the same amount of metals, the different performances should be related to the metal dispersion and/or the nature of active sites. Calcination and reduction at high temperatures lead to a decrease of the nitrate conversion in comparison with the catalysts treated at low temperatures; this can be explained by the decrease of metal surface area due to sintering and/or alloying. Preparation of the catalysts at higher temperatures results in larger metal particles (see Section 3.1.3). Additionally, it was observed by CO adsorption microcalorimetry that heat treatments above 200 °C lead to the formation of an alloy, thus decreasing the number of active sites able to reduce nitrate. Batista et al. [39] and Deganello et al. [58] observed similar performances for nitrate reduction using alloyed or non-alloyed Pd–Cu. On the contrary, our results clearly show that nitrate reduction is highly influenced by the preparation conditions, being the formation of alloys a severe limitation for this reaction. In order to obtain high activities, the metals must be in close contact but not alloyed.

The 2%Pd–1%Cu.ACo catalysts present nitrogen selectivities slightly higher than the 1%Pd–0.3%Cu.ACo catalysts. For the pairs Pd–Cu and Pt–Cu the highest nitrogen selectivities were observed for the catalysts  $T_{\text{Cal}} = 200\text{ °C}$   $T_{\text{Red}} = 200\text{ °C}$ , being the catalysts

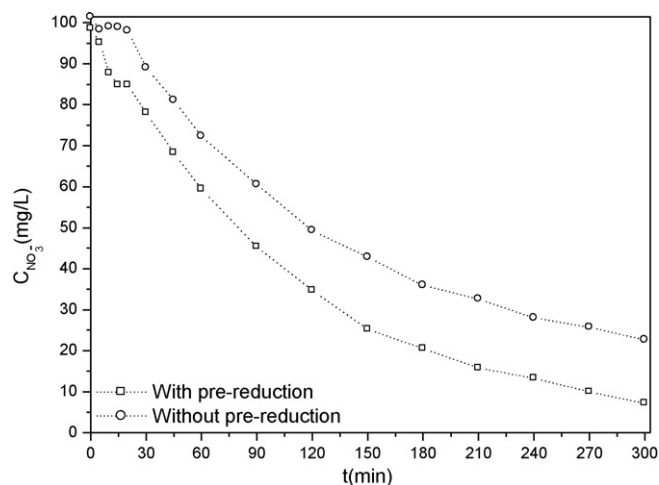


Fig. 9.  $\text{NO}_3^-$  concentration as a function of time during nitrate reduction in the presence of 1%Pd–0.3%Cu.ACo catalysts with and without pre-reduction in water ( $C_{\text{NO}_3^-} = 100\text{ mg/L}$ , catalyst = 0.5 g/L, pH = 5.5,  $Q_{\text{H}_2} = 100\text{ Ncm}^3/\text{min}$ ,  $Q_{\text{CO}_2} = 100\text{ Ncm}^3/\text{min}$ ,  $T = 25\text{ °C}$ ).

$T_{\text{Cal}} = 400\text{ °C}$   $T_{\text{Red}} = 400\text{ °C}$  the most selective to ammonium. Nevertheless, for the Pt–Cu catalysts, the selectivities to nitrogen were not too different from sample to sample. As can be seen in Table 2, the catalysts corresponding to  $T_{\text{Cal}} = 400\text{ °C}$   $T_{\text{Red}} = 400\text{ °C}$  present different nitrate conversions but similar high selectivities to ammonia. According to Sá et al. [37], the decrease in the nitrogen selectivity of the process with the increase of the reduction temperature, can be attributed to alloying of the metals. Yoshinaga et al. [17] suggested that a dilution of Pd takes place during alloying. This leads to an increment in the number of isolated Pd atoms, which are suggested to be active sites for the ammonium formation. In a recent work [23] it was demonstrated that the selectivity to ammonium is higher when the noble metal is isolated, because as the noble metal is very active for hydrogenation reactions the nitrite ions are deeply hydrogenated into ammonium. The pair Pd–Cu is more selective to nitrogen than the pair Pt–Cu. According to this work, the calcination temperature at 200 °C and reduction temperature at 100 °C have been selected as the optimal temperatures for the catalysts activation, in order to achieve reasonable activities and high selectivities to nitrogen. Higher temperatures led to substantial decrease in the catalytic activity probably due to alloy formation and/or sintering, and lower temperatures led to an increase in the catalytic activity but with lower selectivity to nitrogen.

In addition to the metal dispersion, a support promoting effect on the metals may also be considered, since activated carbon has a reducing character, and the contact with hydrogen in water must be considered as an important factor in the catalytic activity. To investigate the influence of passing a hydrogen flow during 15 min before the introduction of nitrates in water in the activity and in the oxidation state of the catalyst, the catalytic reduction of nitrates was performed under different conditions than that normally used. For that purpose, the catalyst (sample 1%Pd–0.3%Cu.ACo  $T_{\text{Cal}} = 200\text{ °C}$   $T_{\text{Red}} = 200\text{ °C}$ ) was only introduced in the reactor together with the concentrated nitrate solution, i.e. after 15 min of flowing hydrogen. Fig. 9 presents the evolution of nitrate concentration in this experiment.

Fig. 9 shows the experiment without *in situ* pre-reduction. The reaction only begins after a period of about 20 min, and a displacement in the corresponding curve relative to that observed for the experiment with pre-reduction was noticed. This induction period can be explained by the time necessary to reduce the noble metal *in situ* with hydrogen and, probably, the presence of hydrogen in water allows a rearrangement of the metal phase, as it has been previously reported by Epron et al. [9]. To confirm this hypothe-

sis, a XPS analysis of the catalyst was carried out after being in contact with hydrogen in water during 15 min. The XPS results (cf. Table 1) lead to the conclusion that the contact with hydrogen in water changes significantly the surface composition of the catalyst. A decrease of the metal surface ratio (Pd/Cu) is observed, probably due to a palladium migration towards the support and/or a migration of copper to the top of palladium. The results obtained permit to conclude that the noble metal can be reduced *in situ* by hydrogen in the presence of activated carbon (avoiding the *ex situ* reducing step).

An additional experiment was carried out to investigate the influence of the contact with dissolved hydrogen in water; the catalyst 1%Pd–0.3%Cu.ACo  $N_{Cal}$   $N_{Red}$  was selected. After a first typical experiment, the catalyst was dried and used again under the same experimental conditions. The results obtained (not shown) demonstrated that in the second run the catalyst is initially more active than in the first experiment, but after 180 min the activity becomes slightly lower. Additionally, it was observed that the selectivity to nitrogen was similar in both experiments. Once again, these results may be interpreted considering that the noble metal was reduced *in situ* by hydrogen and, for that reason, the initial activity is higher in the second test.

#### 4. Conclusions

The results obtained in this work show that the reduction of nitrate is quite different depending on the supported metal and the preparation conditions. For the catalysts tested, the activity decreases with the increase of calcination and reduction temperatures, whereas the effect on the selectivity is not uniform. The calcination and reduction at high temperatures are inadequate due to the formation of larger metal particles and/or alloys. The contact with hydrogen in water has an important effect on the catalytic activity. This contact allows an *in situ* reduction of the noble metal. Taking into consideration the selectivity to nitrogen, the performance of the catalysts is maximised at low calcination and reduction temperatures. The calcination at 200 °C and reduction at 100 °C seem to be the optimal temperatures to activate the catalysts, when both the activity and nitrogen selectivity are considered. For all the preparation conditions tested, the Pd–Cu pair is more selective in the transformation of nitrate into nitrogen.

#### Acknowledgments

This work was carried out with the support of Fundação para a Ciência e a Tecnologia (FCT) and FEDER under programme POCI 2010 and research fellowship BD/30328/2006 and Acção Integrada Luso-Espanhola n.º E31/08–HP2007–0106. Financial support from Generalitat Valenciana (PROMETEO/2009/002) is also gratefully acknowledged.

#### References

- [1] U. Prusse, K.D. Vorlop, Supported bimetallic palladium catalysts for water-phase nitrate reduction, *J. Mol. Catal. A: Chem.* 173 (2001) 313–328.
- [2] A. Pintar, Catalytic processes for the purification of drinking water and industrial effluents, *Catal. Today* 77 (2003) 451–465.
- [3] K.D. Vorlop, T. Tacke, 1st steps towards noble-metal catalyzed removal of nitrate and nitrite from drinking-water, *Chem. Ing. Tech.* 61 (1989) 836–837.
- [4] A. Pintar, J. Batista, J. Levec, Catalytic denitrification: direct and indirect removal of nitrates from potable water, *Catal. Today* 66 (2001) 503–510.
- [5] J. Sá, H. Vinek, Catalytic hydrogenation of nitrates in water over a bimetallic catalyst, *Appl. Catal. B: Environ.* 57 (2005) 247–256.
- [6] F. Gauthard, F. Epron, J. Barbier, Palladium and platinum-based catalysts in the catalytic reduction of nitrate in water: effect of copper, silver, or gold addition, *J. Catal.* 220 (2003) 182–191.
- [7] U. Prusse, M. Hahnlein, J. Daum, K.D. Vorlop, Improving the catalytic nitrate reduction, *Catal. Today* 55 (2000) 79–90.
- [8] I. Witonska, S. Karski, J. Goluchowska, Hydrogenation of nitrate in water over bimetallic Pd–Ag/Al<sub>2</sub>O<sub>3</sub> catalysts, *React. Kinet. Catal. Lett.* 90 (2007) 107–115.
- [9] F. Epron, F. Gauthard, J. Barbier, Influence of oxidizing and reducing treatments on the metal–metal interactions and on the activity for nitrate reduction of a Pt–Cu bimetallic catalyst, *Appl. Catal. A: Gen.* 237 (2002) 253–261.
- [10] A.E. Palomares, C. Franch, A. Corma, Nitrates removal from polluted aquifers using (Sn or Cu)/Pd catalysts in a continuous reactor, *Catal. Today* 149 (2009) 348–351.
- [11] A. Garron, K. Lazar, F. Epron, Effect of the support on tin distribution in Pd–Sn/Al<sub>2</sub>O<sub>3</sub> and Pd–Sn/SiO<sub>2</sub> catalysts for application in water denitration, *Appl. Catal. B: Environ.* 59 (2005) 57–69.
- [12] F.A. Marchesini, S. Iruata, C. Querini, E. Miro, Nitrate hydrogenation over Pt, In/Al<sub>2</sub>O<sub>3</sub> and Pt, In/SiO<sub>2</sub>. Effect of aqueous media and catalyst surface properties upon the catalytic activity, *Catal. Commun.* 9 (2008) 1021–1026.
- [13] F.A. Marchesini, L.B. Gutierrez, C.A. Querini, E.E. Miró, Pt, In, Pd, In catalysts for the hydrogenation of nitrates and nitrites in water. FTIR characterization and reaction studies, *Chem. Eng. J.* (2010) 056, doi:10.1016/j.cej.2010.02.
- [14] H. Berndt, I. Monnich, B. Lucke, M. Menzel, Tin promoted palladium catalysts for nitrate removal from drinking water, *Appl. Catal. B: Environ.* 30 (2001) 111–122.
- [15] J. Sá, C.A. Agüera, S. Gross, J.A. Anderson, Photocatalytic nitrate reduction over metal modified TiO<sub>2</sub>, *Appl. Catal. B: Environ.* 85 (2009) 192–200.
- [16] W.L. Gao, N.J. Guan, J.X. Chen, X.X. Guan, R.C. Jin, H.S. Zeng, Z.G. Liu, F.X. Zhang, Titania supported Pd–Cu bimetallic catalyst for the reduction of nitrate in drinking water, *Appl. Catal. B: Environ.* 46 (2003) 341–351.
- [17] Y. Yoshinaga, T. Akita, I. Mikami, T. Okuhara, Hydrogenation of nitrate in water to nitrogen over Pd–Cu supported on active carbon, *J. Catal.* 207 (2002) 37–45.
- [18] N. Barrabés, J. Just, A. Dafinof, F. Medina, J.L.G. Fierro, J.E. Sueiras, P. Salagre, Y. Cesteros, Catalytic reduction of nitrate on Pt–Cu and Pd–Cu on active carbon using continuous reactor – the effect of copper nanoparticles, *Appl. Catal. B: Environ.* 62 (2006) 77–85.
- [19] L. Lemaignen, C. Tong, V. Begon, R. Burch, D. Chadwick, Catalytic denitrification of water with palladium-based catalysts supported on activated carbons, *Catal. Today* 75 (2002) 43–48.
- [20] Y. Sakamoto, M. Kanno, T. Okuhara, Y. Kamiya, Highly selective hydrogenation of nitrate to harmless compounds in water over copper–palladium bimetallic clusters supported on active carbon, *Catal. Lett.* 125 (2008) 392–395.
- [21] U. Matatov-Meytal, M. Sheintuch, The relation between surface composition of Pd–Cu/ACC catalysts prepared by selective deposition and their denitrification behavior, *Catal. Commun.* 10 (2009) 1137–1141.
- [22] O.S.G.P. Soares, J.J.M. Órfão, M.F.R. Pereira, Activated carbon supported metal catalysts for nitrate and nitrite reduction in water, *Catal. Lett.* 126 (2008) 253–260.
- [23] O.S.G.P. Soares, J.J.M. Órfão, M.F.R. Pereira, Bimetallic catalysts supported on activated carbon for the nitrate reduction in water: optimization of catalysts composition, *Appl. Catal. B: Environ.* 91 (2009) 441–448.
- [24] I. Mikami, Y. Sakamoto, Y. Yoshinaga, T. Okuhara, Kinetic and adsorption studies on the hydrogenation of nitrate and nitrite in water using Pd–Cu on active carbon support, *Appl. Catal. B: Environ.* 44 (2003) 79–86.
- [25] M.P. Maia, M.A. Rodrigues, F.B. Passos, Nitrate catalytic reduction in water using niobia supported palladium–copper catalysts, *Catal. Today* 123 (2007) 171–176.
- [26] A.E. Palomares, J.G. Prato, F. Marquez, A. Corma, Denitrification of natural water on supported Pd/Cu catalysts, *Appl. Catal. B: Environ.* 41 (2003) 3–13.
- [27] Y. Wang, J.H. Qu, H.J. Liu, Effect of liquid property on adsorption and catalytic reduction of nitrate over hydrothermalite-supported Pd–Cu catalyst, *J. Mol. Catal. A: Chem.* 272 (2007) 31–37.
- [28] F. Epron, F. Gauthard, J. Barbier, Catalytic reduction of nitrate in water on a monometallic Pd/CeO<sub>2</sub> catalyst, *J. Catal.* 206 (2002) 363–367.
- [29] N. Barrabés, A. Dafinof, F. Medina, J.E. Sueiras, Catalytic reduction of nitrates using Pt/CeO<sub>2</sub> catalysts in a continuous reactor, *Catal. Today* 149 (2010) 341–347.
- [30] M. D'Arino, F. Pinna, G. Strukul, Nitrate and nitrite hydrogenation with Pd and Pt/SnO<sub>2</sub> catalysts: the effect of the support porosity and the role of carbon dioxide in the control of selectivity, *Appl. Catal. B: Environ.* 53 (2004) 161–168.
- [31] R. Gavagnin, L. Bissetto, F. Pinna, G. Strukul, Nitrate removal in drinking waters: the effect of tin oxides in the catalytic hydrogenation of nitrate by Pd/SnO<sub>2</sub> catalysts, *Appl. Catal. B: Environ.* 38 (2002) 91–99.
- [32] D. Gasparovicova, M. Kralik, M. Hronec, Z. Vallusova, H. Vinek, B. Corain, Supported Pd–Cu catalysts in the water phase reduction of nitrates: functional resin versus alumina, *J. Mol. Catal. A: Chem.* 264 (2007) 93–102.
- [33] C. Neyertz, F.A. Marchesini, A. Boix, E. Miró, C.A. Querini, Catalytic reduction of nitrate in water: promoted palladium catalysts supported in resin, *Appl. Catal. A: Gen.* 372 (2010) 40–47.
- [34] E. Gautron, A. Garron, F. Bost, F. Epron, On the use of polypyrrole-supported Pd–Cu catalysts for nitrate reduction, *Catal. Commun.* 4 (2003) 435–439.
- [35] I. Dodouche, D.P. Barbosa, M.D. Rangel, F. Epron, Palladium–tin catalysts on conducting polymers for nitrate removal, *Appl. Catal. B: Environ.* 93 (2009) 50–55.
- [36] U. Matatov-Meytal, M. Sheintuch, Activated carbon cloth-supported Pd–Cu catalyst: application for continuous water denitrification, *Catal. Today* 102 (2005) 121–127.
- [37] J. Sá, S. Gross, H. Vinek, Effect of the reducing step on the properties of Pd–Cu bimetallic catalysts used for denitration, *Appl. Catal. A: Gen.* 294 (2005) 226–234.

- [38] F. Rodríguez-Reinoso, The role of carbon materials in heterogeneous catalysis, *Carbon* (1998) 159–175.
- [39] J. Batista, A. Pintar, D. Mandrino, M. Jenko, V. Martin, X.P.S. TPR, examinations of gamma-alumina-supported Pd–Cu catalysts, *Appl. Catal. A: Gen.* 206 (2001) 113–124.
- [40] M. Gurrath, T. Kuretzky, H.P. Boehm, L.B. Okhlopkova, A.S. Lisitsyn, V.A. Likhobolov, Palladium catalysts on activated carbon supports - Influence of reduction temperature, origin of the support and pretreatments of the carbon surface, *Carbon* 38 (2000) 1241–1255.
- [41] C.M. Mendez, H. Olivero, D.E. Damiani, M.A. Volpe, On the role of Pd beta-hydride in the reduction of nitrate over Pd based catalyst, *Appl. Catal. B: Environ.* 84 (2008) 156–161.
- [42] E.A. Sales, T.R.O. de Souza, R.C. Santos, H.M.C. Andrade, N<sub>2</sub>O decomposition coupled with ethanol oxidative dehydrogenation reaction on carbon-supported copper catalysts promoted by palladium and cobalt, *Catal. Today* 107–08 (2005) 114–119.
- [43] A.L.D. Ramos, P.D. Alves, D.A.G. Aranda, M. Schmal, Characterization of carbon supported palladium catalysts: inference of electronic and particle size effects using reaction probes, *Appl. Catal. A: Gen.* 277 (2004) 71–81.
- [44] A. Sepúlveda-Escribano, F. Coloma, F. Rodríguez-Reinoso, Platinum catalysts supported on carbon blacks with different surface chemical properties, *Appl. Catal. A: Gen.* 173 (1998) 247–257.
- [45] F. Coloma, J. Narciso-Romero, A. Sepúlveda-Escribano, F. Rodríguez-Reinoso, Gas phase hydrogenation of crotonaldehyde over platinum supported on oxidized carbon black, *Carbon* 36 (1998) 1011–1019.
- [46] C. Crisafulli, S. Galvagno, R. Maggiore, S. Scire, A. Saeli, Performance of supported Ru–Cu bimetallic catalysts prepared from nitrate precursors, *Catal. Lett.* 6 (1990) 77–83.
- [47] C.P. Vinod, K.R. Harikumar, G.U. Kulkarni, C.N.R. Rao, Interaction of carbon monoxide with Cu–Pd and Cu–Ni bimetallic clusters, *Top. Catal.* 11 (2000) 293–298.
- [48] M. Fernandez-Garcia, J.A. Anderson, G.L. Haller, Alloy formation and stability in Pd–Cu bimetallic catalysts, *J. Phys. Chem.* 100 (1996) 16247–16254.
- [49] J.A. Anderson, M. Fernandez-Garcia, G.L. Haller, Surface and bulk characterization of metallic phases present during CO hydrogenation over Pd–Cu/KL zeolite catalysts, *J. Catal.* 164 (1996) 477–483.
- [50] A. Guerrero-Ruiz, S.W. Yang, Q. Xin, A. Maroto-Valiente, M. Benito-Gonzalez, I. Rodriguez-Ramos, Comparative study by infrared spectroscopy and microcalorimetry of the CO adsorption over supported palladium catalysts, *Langmuir* 16 (2000) 8100–8106.
- [51] L. Li, X.D. Wang, A.Q. Wang, J.Y. Shen, T. Zhang, Relationship between adsorption properties of Pt–Cu/SiO<sub>2</sub> catalysts and their catalytic performance for selective hydrodechlorination of 1,2-dichloroethane to ethylene, *Thermochim. Acta* 494 (2009) 99–103.
- [52] A. Manivannan, M. Chirila, N.C. Giles, M.S. Seehra, Microstructure, dangling bonds and impurities in activated carbons, *Carbon* 37 (1999) 1741–1747.
- [53] R.M. Navarro, M.A. Pena, C. Merino, J.L.G. Fierro, Production of hydrogen by partial oxidation of methanol over carbon-supported copper catalysts, *Top. Catal.* 30–31 (2004) 481–486.
- [54] Z.F. Wang, W.P. Wang, G.X. Lu, Studies on the active species and on dispersion of Cu in Cu/SiO<sub>2</sub> and Cu/Zn/SiO<sub>2</sub> for hydrogen production via methanol partial oxidation, *Int. J. Hydrogen Energy* 28 (2003) 151–158.
- [55] M. Brun, A. Berthet, J.C. Bertolini, XPS, AES and Auger parameter of Pd and PdO, *J. Electron. Spectrosc. Relat. Phenom.* 104 (1999) 55–60.
- [56] K.S. Kim, A.F. Gossmann, N. Winograd, X-ray photoelectron spectroscopic studies of palladium oxides and palladium–oxygen electrode, *Anal. Chem.* 46 (1974) 197–200.
- [57] Y. Yamamoto, T. Matsuzaki, K. Ohdan, Y. Okamoto, Structure and electronic state of PdCl<sub>2</sub>–CuCl<sub>2</sub> catalysts supported on activated carbon, *J. Catal.* 161 (1996) 577–586.
- [58] F. Deganello, L.F. Liotta, A. Macaluso, A.M. Venezia, G. Deganello, Catalytic reduction of nitrates and nitrites in water solution on pumice-supported Pd–Cu catalysts, *Appl. Catal. B: Environ.* 24 (2000) 265–273.